RSC Advances

ROYAL SOCIETY OF CHEMISTRY

www.rsc.org/advances

Large Scale Bi-layer Graphene by Suppression of Nucleation from Solid Precursor

Mohsin Ahmed[1]*, Naoki Kishi[1], Tetsuo Soga[1]

[1]Department of Frontier Materials, Nagoya Institute of Technology, Nagoya 466-8555, Japan.

*Corresponding author :mohsin94ee@yahoo.com

Abstract: We report synthesis of large-scale Bilayer Graphene (BLG) from solid precursor, camphor using Chemical Vapor Deposition (CVD) method at atmospheric pressure. Controlled insertion of carbon source was obtained by two-fold gas flow approach and found to haveprofound impact to obtain continuous BLG. Suppression of nucleation by annealing the substrate for extended period helped to obtain large scale BLG on Cooper foil. The impact of deposition temperature, deposition time, flow of carrier gas were examined for further optimization. The as grown BLGwas transferred to insulator substrate and measured transmittance was found above 90%. This mechanism to obtain low cost BLG in large scale may have profound implications in semiconductor industries.

Keyword: Bilayer Graphene (BLG), Chemical Vapor Deposition(CVD),Botanic precursor, Suppression of nucleation.

Introduction:

Graphene is the hexagonal lattice structured sp^2 bonded network of carbon with extraordinary electron mobility. However, the promise and novelty of graphene is yet to be exploited to its highest level due to its zero band-gap property.The absence of a band gap limits thetypes of electronic devices that can be developed from graphene.Graphene-based transistors with very high operating frequency requiringvery low input power have the limitation of poor control over the carrier concentrations due to the inability to turn off the RF transistors(1-3). Therefore, opening a band gap in graphene has become very crucialin the field of graphene based electronic applications(4-6).For the band gap opening,several attempts have been envisaged by confining carriers physically,such as,patterning graphene into graphene nanoribbons (GNR)(7, 8) or unzipping carbon nanotubes (CNTs) into GNRs(9). Nevertheless, those methods are quite challenging as precise control of the width and edge roughness of nanometer-width GNRs or exact alignment of CNTs on the substrate is required.

The bandgap opening has been done in recent years in Bernal (AB) stacked bilayer graphene by breaking symmetry of the electron wave functions(10-12).To introduce a gap between the Π and Π* states in graphene, the lattice symmetry in hexagonal structured graphene needs to be broken down. If two layers of graphene are stacked as in graphite and both graphene layers are yielded in-equivalent, an energy gap between low-energy bands is formed. It was demonstrated that, by controlling the carrier density in a bilayer graphene, the position of electronic states near E_F and the magnitude of the gap between the VB and CB can be manipulated(13).The change in the charge state i.e positioning of E_F within the gap causes a semimetal-to-insulator transition. If this symmetry-breaking could be

controlled externally, the electronic conductivity would change through this transition, suggesting that a switch with a thickness of two atomic layers could be constructed(14). Thus, the opening of bandgap and its tunable criteria provide immense opportunity for BLG to be used in electronic and photonic devices(15-17).

Applications of BLG vastly depend on scalability and quality of the synthesized graphene(18). Up to now,mechanical exfoliation method was utilized mostly to fabricate AB stackedBLG(19-21).However, exfoliated graphenes are limited in size and not scalable. Recent advancement in CVD technology has paved the way to synthesis scalable graphene.This technique has proved to be effective in controlling number of graphene layers and stacking orderand hence, spurred large-scale production of AB stacked bilayer graphene for numerous applications(22).

Transition metals, such as Ni and Cuhave been exploited mostly to synthesis graphene by CVD technique.It is quite challenging to produce BLG on Ni due to high carbon solubility and graphene grown on Ni (23)lacking uniformity. On the other hand, exploitation of BLG on Cu is critical because of Cu's weak capability of decomposing hydrocarbons (24, 25) which makes this transition metal self-limiting. At the same time, self-limiting criteria of Cu is crucial to obtain continuous BLG which is difficult to achieve on Ni.In order to prepare BLG on Cu foils, the self-limiting growth process needs to be controlled precisely by adopting some methods,such as using Cu-Ni alloy, low-pressure synthesis and controlling the graphene nucleation on Cu.In recent times, BLG with high coverage has been prepared on engineered Cu–Ni alloy films. (16) which requires a hectic process of controlling composition of Cu,Ni and appropiate condition for BLG growth.Z.Sun et al. showed that BLG could

be grown by precisely tuning the the pressure in the CVD chamber(26).BLG obtained by this approach still has some patches of tri-layer and tetralayer.In obtaining uniformity in single and bilayer graphene,purity of Cu substrate along with partial pressure of hydrocarbon was identified as the key factor by Wei Liu et al.(22). In recent years, suppression of nucleation has been emphasized to achieve large-scale graphene on Cu substrate (27). However, most of the studies in this approach were based on obtaining single layer Graphene. Suppression of nucleation plays a pivotal role in the creation of uniform nucleation over the substrate and obtains maximum coverage of the single layer graphene(28).However, the impact of suppressing nucleation on forming BLG has not been reported up to now.

In this work, controlled nucleation for an extended period with low concentration of precursor was adopted to synthesize continuous BLG. Solid botanical derivative ($C_{10}H_{16}O$), a green and renewable carbon source was used as precursor to obtain low cost continuous BLG. We used two-way gas flow to the CVD chamber to obtain greater control over deposition. Using the solid carbon source, the effect of other growth parameters such as temperature and deposition time was investigated and optimized.

2. Experimental details:

Polycrystalline Cu foil, purchased from Nilaco Corporation of 99% purity and 25μm thickness was cut into 1cm×2 cm and 5mm×5mm pieces. A long quartz tube 120 cm long and 75 mm in diameter was made for the CVD experiment. Besides, a precursor chamber made of glass was used to introduce carbon source and to facilitate its controlled insertion for reaction with substrate. Two separately

controlled furnaces, one for the precursor chamber (furnace 1) and one for placing the substrate (furnace 2) were used at the same time. Argon and hydrogen with a ratio of 3:1 and purity of 99% were used to transport the camphor precursor to react with Cu foil placed in furnace 2. Flow of precursor to the substrate was tuned by two-way flow of carrier gas ($Ar+H_2$); one way was carrier gas to the substrate through precursor chamber (F2) and another was through the quartz tube only (F1).

Cu substrates were cleaned by sonication for 5 minutes in acetone, then rinsed in methanol followed by isopropanol, and then loaded into quartz tube furnace.The substrate was annealed at 1000°C for 60 minutes before deposition. A wide range of temperature ranging from 950°C to 1050°Cwas chosen in the current approach whereas,deposition time varied from 5 to 30 minutes.The precursor chamber was placed in the center of the furnace set at 85-110°C. The flow rate of $Ar+H_2$was precisely controlled from 6-18sccm inside the quartz tube (F1) and 2-6sccm inside the precursor chamber (F2). Rapid cooling was performed(29) immediately after the deposition. As-grown samples were characterized by Field Emission Scanning Electron Microscopy (FESEM,JEOL JSM -7001FF), Raman Spectroscopy (green laser with excitation wavelength of 532 nm, JASCO NRS-1500W) and Raman mapping by NRS-3300, Transmission Electron Microscopy (TEM) by JEM-2100F by JEOL and UV–visible spectrophotometer measured by V-570, JASCO.

Result and Discussion:

In our approach, we reduced the intensity of nucleation of carbon on the Cu substrate and obtained controlled growth by changing the carrier gas and carbon source insertion. This was accomplishedby

varying the temperature of furnace 1 in the range of 80-110°C .Further control over the flow of precursor was maintained by controlling F2 and F1, shown in figure 1.

Raman spectroscopy and Raman mapping were carried out to characterize as grown deposition. Raman spectroscopy is a simple technique that uses the Raman scattering phenomena to evaluate the quality and justify the number of layers of graphene. The strongest Raman peaks in crystalline graphene are G (~1584 cm^{-1}) and 2D (~2400-2800 cm^{-1}) bands(30).Furthermore, the existence of disorder in the graphene lattice causes the appearance of so-called D bands (~1200-1400 cm^{-1}). The ratio of 2D and G peak (I_{2D}/I_G) and the Full Width Half maximum (FWHM) of the 2D peak can be used to evaluate the number of graphene layers(31). The value of I_{2D}/I_G more than 1 and FWHM value less than 30 cm^{-1} indicates single layer graphene structure whereas for multilayer graphite, $I_{2D}/I_G>1$ and FWHM ~40 cm^{-1}(32).Besides, the ratio of G to D peak (I_G/I_D) determines the quality and disorder in graphene(21, 32).

Raman spectroscopic information in figure 2(a-b) shows that the proportion of carrier gas flow to the precursor chamber (F2) and the quartz tube (F1) has significant impact on formation of bilayer graphene. These two flow rates were tuned while temperature, pressure and deposition time were keptconstant at 1050°C, 1 atmospheric pressure and 30 minutes respectively.Figure 2(a) shows that while flow rate, F1 remained unchanged, changing flow rate, F2 impacts graphene deposition. When F2 and F1 are equal(F2, F1- 2 and 2 sccm respectively), a very low intensity G and 2D peak are observed. As the F2:F1 is soared up to 2 (F2 and F1- 2 and 4 sccm respectively), intense G peak along with defective D and 2D band are observed (i.e. $I_{2D}/I_G<1$) which indicates existence of few layer

graphene with substantial defects. As F1 is increased further(F1=6sccm), 2D and G peak with equal intensity are observed which justify BLG. Catalytic reaction of Cu with carbon vastly depends on carrier gas and precursor composition(24). It can be seen that for F2:F1 at minimum value ensures less amount of precursor to react with Cu per unit of time which contributes some small patches of carbon on Cu with less significant D,G and 2D peak.Constant precursor gas flow,F2 and further increase of carrier gas flow,F1cause more carbon to react in a given time and hence gives few graphene layers with significant defectivity. As the F2:F1 is made 2:6, uniform catalytic reaction on Cu takes place which contributes to the formation of BLG. Furthermore, higher carrier gas flow, F1 may lead to high desorption rate and hence, reduce formation of multilayer graphene on Cu. An opposite attempt, increasing F2 and keeping F1 fixed is proven to be detrimental to obtain uniform BLG, shown in figure 2(b).For the flow ratio, F1:F2 = 6:6 , the G peak is seen to be slightly higher than 2D (I_{2D}/I_G <1).As the proportion of F2 and F1 become 12:6, intensity of G peak becomes more intense, compared to 2D, which proves multilayer graphene. More intense G peak , almost twice of the 2D peak is observed while F2 and F1 become 18 sccm and 6 sccm respectively. Keeping carrier gas flow F1 at constant value and increasing precursor gas flow, F2 allows more adsorption than desorption and hence contributesformation of more layers. It is interesting to observe that at high F2:F1, D peak diminishes, shownin figure 2(b). As the deposition shows more graphitic pattern, the defect reducedsignificantly(33).

Deposition temperature has vast impact on obtaining larger flakes. In figure 2 (c-e), FESEM images illustrate the impact of temperature on formation of larger flakes of graphene on Cu foil. A low influx

of precursor was maintained by ensuring a low F2(2 sccm) and moderate F1(6 sccm) to the CVD furnace for 30 minutes deposition at three different temperatures(950°C,1000°C and 1050°C) and atmospheric pressure. It can be seen from figure 2(c), at deposition temperature of 950°C, very few hexagon-shaped sites are observed indicated by white arrows. As the deposition temperature is raised to 1000°C, more hexagonal shapes are visualized, shown in figure 2(d). At 1050°C, the graphene structure spreads over the whole substrates, shown in figure 2(e).Thus,it is obvious that deposition at high temperature affects flakes size of graphene on Cu substrates.

According to the relation between diffusivity of carbon and temperature, it can be seen:

$$D_C = D_C^o \, exp^{(\frac{-Q_D}{RT})} \qquad (1)$$

Where, R is the universal gas constant, Q_D is the activation energy for diffusion and Dc is the diffusion constant respectively. It can be deduced from the equation that higher temperature enhances the diffusivity of carbon on the Cu foil.As the growth temperature increases,the concentration of the active carbon species on the surface reduces by enhancement of desorption(34). In adddition,the higher annealing temperature improves the quality of Cu substartes(35).Therefore, for an extended growth period,the domain size of graphene increases.Therefore, it can be concluded that as we allowed very small amount of carbon source to react with Cu, increased the deposition temperature as well as extended deposition time, the suppression of nucleation helped to obtain larger flakes of graphene.Quite a few white spots are visualized which are Cu nanoparticles described elsewhere(36).

In figure 3(a-f),it is observed from Raman mapping that deposition for an extended period helps to attain more BLG than deposition for small duration. The deposition temperature and pressure were kept at 1050°C and 1 atmospheric pressure respectively with low insertion of precursor(F2:F1=2:6) by two way carrier gas flow. For the deposition time of 5 minutes, it is seen that I_{2D}/I_G varies from 0.2 to 1.5, shown in figure 3(a).For 15 minutes deposition(shown in figure 3b), $I_{2D}/I_G$is observed to be confined to the range of 0.4 to1.2 which indicates existence of mostlyBLG. As the deposition time is further increased to 30 minutes, 2D to G peak ratio becomes limited to the range of 0.9 to 1.2 (shown in figure 3(c)) which validates that extended period of deposition contributes more BLG sites. In figure 3(d-f), the graph of I_{2D}/I_G vs FWHM was plotted, considering 100 points from the substrates (shown in figure 3(a-c)).Figure 3(d) represents indiscriminate scattering of graphene/graphitic sites for the deposition of 5 minutes, where scattering of I_{2D}/I_G and FWHM ranges from 0.2 to 1.3 and 25 to 65 cm^{-1} respectively which indicates single to few layer graphene existence. Less dispersion is seen for the deposition of 15 minutes, illustrated in figure 3(e).It is visualized that the point of graphitization tends to locate near the range of 0.6-1.0 for I_{2D}/I_G and 40-50cm^{-1} for FWHM which suggests more BLG for deposition for extended period. This spreading phenomenon is significantly reduced when the deposition time was extended for 30 minutes, shown in figure 3(f).For less deposition time, a small number of carbon particles are involved in diffusion with less nucleation sites. Therefore, single to few layer graphene is formed in those nucleated points .Deposition for extended time (15-30 minutes) contributes more nucleation sites which are distributed almost equally over the substrate and hence impart uniform diffusion of carbon. Formation of BLG initiates from the SLG flakes and

largely depends on coverage of SLG on the substrate and the deposition time (37). As the precursor reacts with Cu and deposition of monolayer is yet to be completed ,the deposition of bilayer starts from the middle of the monolayer flakes,shown in figure 4(a-b).Even,after the completion of full coverage of monolayer formation(shown in figure 4(c)) on substrate,bilayer formation goes on. Therefore,extended period of deposition helps to form continuous BLG on Cu substarte(figure 4(d)).

It is also observed that deposition for extended period helps to reduce defects significantly in the suppression of nucleation approach. It is important to note that ratio of G to D depicts the defects, graphitization as well as crystallite dimension(38). Here, low insertion of precursor(F2:F1=2:6) was maintained while deposition temperature and pressure were kept at 1050°C and 1 atmospheric pressure respectively.In Figure 5(a-c), spatial representation of G to D ratio (I_G/I_D) shows that deposition with a short period contributes lower G to D ratio whereas, long-duration growth provides comparatively high G to D ratio .It can be seen from figure 5(a), the I_G/I_D ratio varies in the range of 0.7 to 3.3 for the deposition of 5 minutes which proves existence of substantial defects along with graphitization.Deposition for 15 minutes demonstrates more graphitization sites as I_G/I_D ranges from 1 to 7.For an extended period of 30 minutes, the peak intensity ratio of G to D varies from 3 to 7 which further proves more graphitization for the deposition of longer period. It is clear that higher deposition time is vital to obtain more graphitic carbon with the suppression of nucleation approach.

It is well known that the I_G/I_D gives a glimpse of grain size of the flakes. According to the Tuinstra-Koenig(39) relationship:

$$\frac{I_G}{I_D} = L_a/(C\lambda)\text{……..(2)}$$

Where, I_G and I_D is the ratio of G and D peak respectively and La is the crystallite size. As the ratio (I_G /I_D) increases, the crystallite size increases. By comparing Figure 5(a-c), it can be inferred that for an extended duration of deposition, the I_G/I_D becomes higher compared to the deposition of shorter period and hence gives larger flakes.

To investigate the coverage of graphitization and continuity of BLGby suppression of nucleation, Raman mapping was performed in three different sites (27 μm x 27 μm each, shown in figure 5(d)) of samples annealed for 5,15 and 30 minutes at 1050 °C with low insertion of precursor(F2:F1=2:6). Extracted I_G/I_D, I_G/I_D deviation and deposition time were plotted, shown in figure 5(e). It can be seen from figure 5(e) that average I_G/I_D for the mapped three areas is much lower for 5 minutes deposition and increased significantly for the long period of deposition which is clearly in agreement with the previous claim of better graphitization for the deposition of extended period.In figure 5(f), it isobserved that deposition for extended time is crucial to obtain continuous BLG. ExtractedI_{2D}/I_G and deviation of I_{2D}/I_G from the three mapped areas areplotted against deposition time. It is observed that I_{2D}/I_G deviation is much higher for deposition of short period where as for extended time, the deviation reduced significantly along with escalation of I_{2D}/I_Gvalue. Thus, it further proves that deposition for long time helps the growth of BLG in the current approach of suppression of nucleation.

The stacking structure of graphene film was studied by TEM measurement, shown in figure 6(a-b) which further confirmed the existence of BLG. The film was transferred on TEM grid and existence of graphene was confirmed the by Raman spectroscopy. As shown in the figure 6(a), in the TEM grid, investigated portion of the film is shown by an arrow. A high-resolution TEM image is taken, shown in Figure 6(b).The inset image shows the diffraction pattern of graphene displays hexagonal crystalline structure. The calculated interlayer spacing of the graphene is about 0.34 nm, shown in figure 6(b).In the TEM image, most of the layer observed are bi-layer providing clear evidence of bi-layer deposition.

Graphene with tunable properties and flexible criteria has numerous applications (40, 41)**.**In the current approach, the deposited graphene was transferred from Cu foil to an insulator substrate, silicone rubber (polymerized siloxanes), shown in figure 7(a-d). Silicone Rubber (SR) has transparent and flexible properties. At first, Graphene on Cu was hot pressed with SR at moderate temperature and pressure(shown in figure 7(a-b)). The Cu/BLG/SR structure was submerged into diluted HNO_3 for 24 hours and the metal was etched (shown in figure 7(c-d)). Figure 7(e) shows Raman spectroscopic information depicting quality of BLG before and after transfer process. As-grown BLG on Cu shows almost no D peak, whereas, after the transfer on SR, small D peak is observed. Chemical etching is supposed to impart small defects on BLG on SR. The measured transmittance of graphene on silicon rubber is ~93% in the visible region (as shown in figure 7(f)) ,whereas inset image shows transferred graphene on SR which further validates our stance of synthesis of large scale BLG.

Conclusion:

We synthesized large scale BLG from botanic precursor, camphor. Continuous bilayer was obtained by two-way carrier gas insertion, which has proven instrumental in obtaining much control over BLG growth. The deposition by suppressing the flow of carbon source to CVD chamber providedBLGwith large flakes. It was also found that deposition of long duration and deposition temperature are crucial to reduce the defects in the film and increase the grain size too. Transferred bilayer in flexible and transparent silicones substrates provided high transmittance in the visible region. Our approach, continuous BLG from solid precursorsis cost efficient and highly controllable and may have vast implications in electronic industries.

Reference:

1. Schwierz F. Graphene transistors. Nat Nanotechnol. 2010;5(7):487-96.
2. Dimitrakopoulos C, Lin Y-M, Grill A, Farmer DB, Freitag M, Sun Y, et al. Wafer-scale epitaxial graphene growth on the Si-face of hexagonal SiC (0001) for high frequency transistors. Journal of Vacuum Science & Technology B. 2010;28(5):985-92.
3. Dragoman M, Neculoiu D, Deligeorgis G, Konstantinidis G, Dragoman D, Cismaru A, et al. Millimeter-wave generation via frequency multiplication in graphene. Applied Physics Letters. 2010;97(9):093101.
4. Han MY, Özyilmaz B, Zhang Y, Kim P. Energy Band-Gap Engineering of Graphene Nanoribbons. Physical Review Letters. 2007;98(20):206805.
5. Zhang Y, Tang T-T, Girit C, Hao Z, Martin MC, Zettl A, et al. Direct observation of a widely tunable bandgap in bilayer graphene. Nature. 2009;459(7248):820-3.
6. Wang X, Ouyang Y, Li X, Wang H, Guo J, Dai H. Room-Temperature All-Semiconducting Sub-10-nm Graphene Nanoribbon Field-Effect Transistors. Physical Review Letters. 2008;100(20):206803.
7. Dvorak M, Oswald W, Wu Z. Bandgap Opening by Patterning Graphene. Sci Rep. 2013;3.
8. Balog R, Jorgensen B, Nilsson L, Andersen M, Rienks E, Bianchi M, et al. Bandgap opening in graphene induced by patterned hydrogen adsorption. Nat Mater. 2010;9(4):315-9.
9. Jiao L, Zhang L, Wang X, Diankov G, Dai H. Narrow graphene nanoribbons from carbon nanotubes. Nature. 2009;458(7240):877-80.

10. Park J, Jo SB, Yu Y-J, Kim Y, Yang JW, Lee WH, et al. Single-Gate Bandgap Opening of Bilayer Graphene by Dual Molecular Doping. Advanced Materials. 2012;24(3):407-11.

11. Wang TH, Zhu YF, Jiang Q. Bandgap Opening of Bilayer Graphene by Dual Doping from Organic Molecule and Substrate. The Journal of Physical Chemistry C. 2013;117(24):12873-81.

12. Samuels AJ, Carey JD. Molecular Doping and Band-Gap Opening of Bilayer Graphene. ACS Nano. 2013;7(3):2790-9.

13. Shinichi Tanabe YS, Hiroyuki Kageshima, Masao Nagase and Hiroki Hibino. Observation of Band Gap in Epitaxial Bilayer Graphene Field Effect Transistors. Jpn J Appl Phys 2011;50: 04DN.

14. Ohta T. BA, Seyller T, Horn K and Rotenberg E. Controlling the electronic structure of bilayer graphene. Science. 2006;313:951.

15. Avouris P. Graphene: Electronic and Photonic Properties and Devices. Nano Letters. 2010;10(11):4285-94.

16. Xia F, Mueller T, Lin Y-m, Valdes-Garcia A, Avouris P. Ultrafast graphene photodetector. Nat Nano. 2009;4(12):839-43.

17. Chen Y, Zhang B, Liu G, Zhuang X, Kang E-T. Graphene and its derivatives: switching ON and OFF. Chemical Society Reviews. 2012;41(13):4688-707.

18. Schwierz F. Graphene transistors. Nat Nano. 2010;5(7):487-96.

19. Liu W, Kraemer S, Sarkar D, Li H, Ajayan PM, Banerjee K. Controllable and Rapid Synthesis of High-Quality and Large-Area Bernal Stacked Bilayer Graphene Using Chemical Vapor Deposition. Chemistry of Materials. 2014;26(2):907-15.

20. Liu W, Li H, Xu C, Khatami Y, Banerjee K. Synthesis of high-quality monolayer and bilayer graphene on copper using chemical vapor deposition. Carbon. 2011;49(13):4122-30.

21. Lee S, Lee K, Zhong Z. Wafer Scale Homogeneous Bilayer Graphene Films by Chemical Vapor Deposition. Nano Letters. 2010;10(11):4702-7.

22. Wei Liu HL, Chuan Xu, Yasin Khatami, Kaustav Banerjee Synthesis of high-quality monolayer and bilayer graphene on copper using chemical vapor deposition. CARBON. 2011;49:4122 – 30.

23. Liu W, Chung C-H, Miao C-Q, Wang Y-J, Li B-Y, Ruan L-Y, et al. Chemical vapor deposition of large area few layer graphene on Si catalyzed with nickel films. Thin Solid Films. 2010;518(6, Supplement 1):S128-S32.

24. Bhaviripudi S, Jia X, Dresselhaus MS, Kong J. Role of Kinetic Factors in Chemical Vapor Deposition Synthesis of Uniform Large Area Graphene Using Copper Catalyst. Nano Letters. 2010;10(10):4128-33.

25. Gao L, Ren W, Xu H, Jin L, Wang Z, Ma T, et al. Repeated growth and bubbling transfer of graphene with millimetre-size single-crystal grains using platinum. Nat Commun. 2012;3:699.

26. Sun Z, Raji A-RO, Zhu Y, Xiang C, Yan Z, Kittrell C, et al. Large-Area Bernal-Stacked Bi-, Tri-, and Tetralayer Graphene. ACS Nano. 2012;6(11):9790-6.

27. Zhan D, Yan JX, Ni ZH, Sun L, Lai LF, Liu L, et al. Bandgap-Opened Bilayer Graphene Approached by Asymmetrical Intercalation of Trilayer Graphene. Small. 2015;11(9-10):1177-82.

28. Seiya Suzuki TN, Yuki Matsuoka and Masamichi Yoshimura. Threefold atmospheric-pressure annealing for suppressing graphene nucleation on copper in chemical vapor deposition. Jpn J Appl Phys. 2014;53:095101.

29. Li X, Magnuson CW, Venugopal A, Tromp RM, Hannon JB, Vogel EM, et al. Large-Area Graphene Single Crystals Grown by Low-Pressure Chemical Vapor Deposition of Methane on Copper. Journal of the American Chemical Society. 2011;133(9):2816-9.

30. Ferrari AC, Basko DM. Raman spectroscopy as a versatile tool for studying the properties of graphene. Nat Nano. 2013;8(4):235-46.

31. Ivan Vlassiouk SS, Ilia Ivanov, Pasquale F Fulvio, Sheng Dai, Harry Meyer, Miaofang Chi, Dale Hensley, Panos Datskos and Nickolay V Lavrik. Electrical and thermal conductivity of low temperature CVD graphene: the effect of disorder. Nanotechnology. 2011;22:275716.

32. Yan K, Peng H, Zhou Y, Li H, Liu Z. Formation of Bilayer Bernal Graphene: Layer-by-Layer Epitaxy via Chemical Vapor Deposition. Nano Letters. 2011;11(3):1106-10.

33. Jorio A, Ferreira EHM, Moutinho MVO, Stavale F, Achete CA, Capaz RB. Measuring disorder in graphene with the G and D bands. physica status solidi (b). 2010;247(11-12):2980-2.

34. Kim H, Mattevi C, Calvo MR, Oberg JC, Artiglia L, Agnoli S, et al. Activation Energy Paths for Graphene Nucleation and Growth on Cu. ACS Nano. 2012;6(4):3614-23.

35. Ajmal M, Lee S, Cho YC, Kim SJ, Park SE, Cho CR, et al. Fabrication of the best conductor from single-crystal copper and the contribution of grain boundaries to the Debye temperature. Cryst Eng Comm. 2012;14(4):1463-7.

36. Fan L, Wang K, Wei J, Zhong M, Wu D, Zhu H. Correlation between nanoparticle location and graphene nucleation in chemical vapour deposition of graphene. Journal of Materials Chemistry A. 2014;2(32):13123-8.

37. Fang W, Hsu AL, Song Y, Birdwell AG, Amani M, Dubey M, et al. Asymmetric Growth of Bilayer Graphene on Copper Enclosures Using Low-Pressure Chemical Vapor Deposition. ACS Nano. 2014;8(6):6491-9.

38. M. A. Pimenta GD, M. S. Dresselhaus,L. G. Canc¸ado,, Saito AJaR. Studying disorder in graphite-based systems by Raman spectroscopy. Phys Chem Chem Phys. 2007;9:1276–91.

39. Tuinstra F, Koenig JL. Raman Spectrum of Graphite. The Journal of Chemical Physics. 1970;53(3):1126-30.

40. Seunghyun Lee KL, Chang-Hua Liu and Zhaohui Zhong. Homogeneous bilayer graphene film based flexible transparent conductor. Nanoscale. 2012;4:639.

41. Martins LGP, Song Y, Zeng T, Dresselhaus MS, Kong J, Araujo PT. Direct transfer of graphene onto flexible substrates. Proc Natl Acad Sci U S A. 2013;110(44):17762-7.

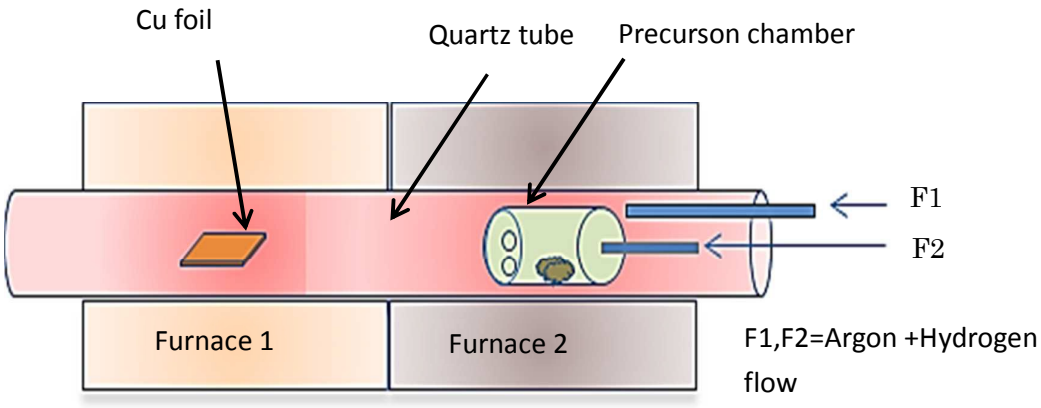

Figure 1: Schematic diagram of two-furnace set side by side along with special arrangement of precursor chamber to control precursor flow.

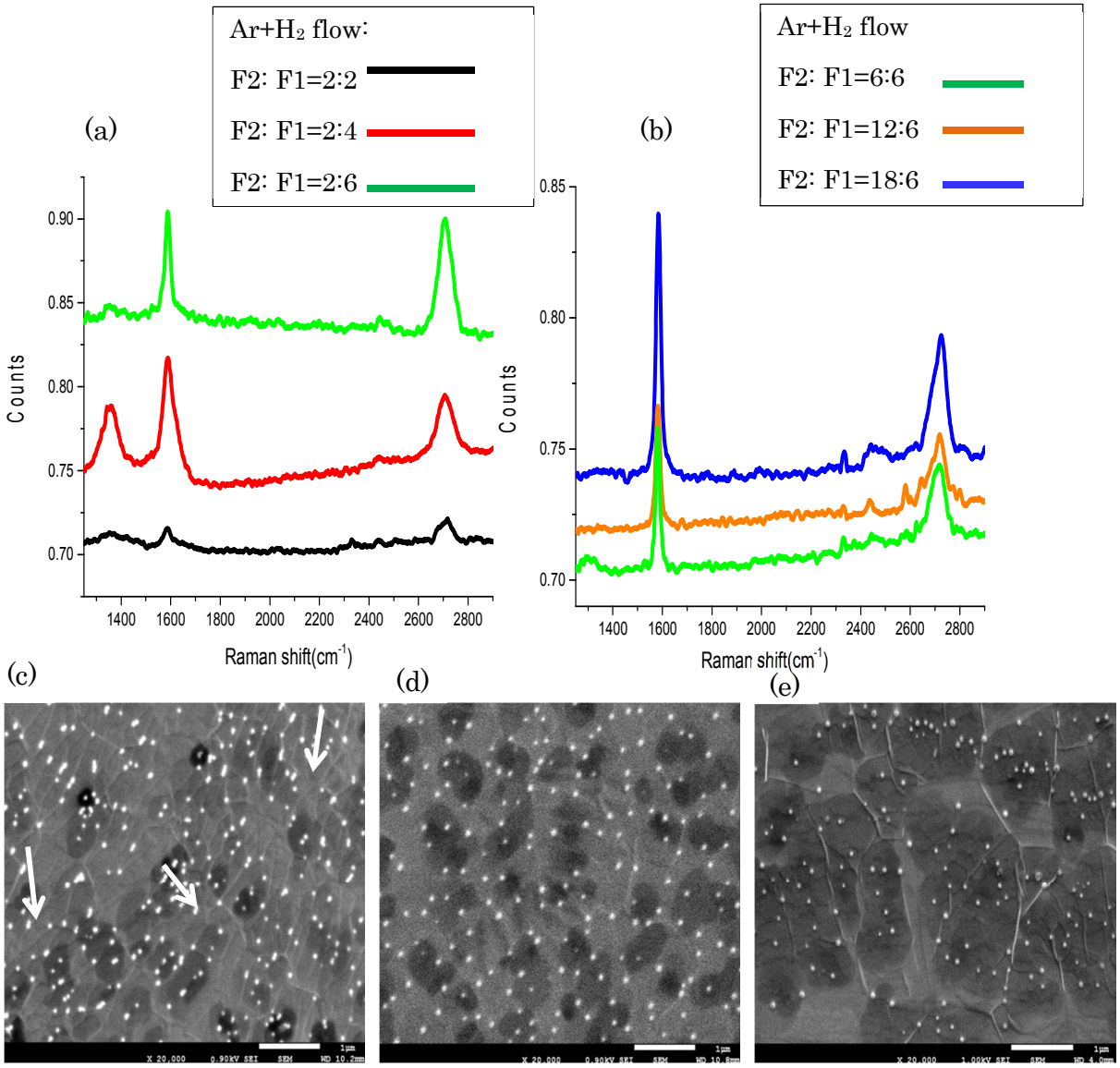

Figure 2,Raman spectroscopy for varying gas flow;(a) Impact due to changing gas flow to quart(F1),(b) Graphene formation due to the variation in carrier gas flow to precursor chamber(F2), FESEM image of different temperature.Deposition at (c) 950°C (d)1000°C and (e)1050°C shows that increasing deposition temperature increases flakes size.

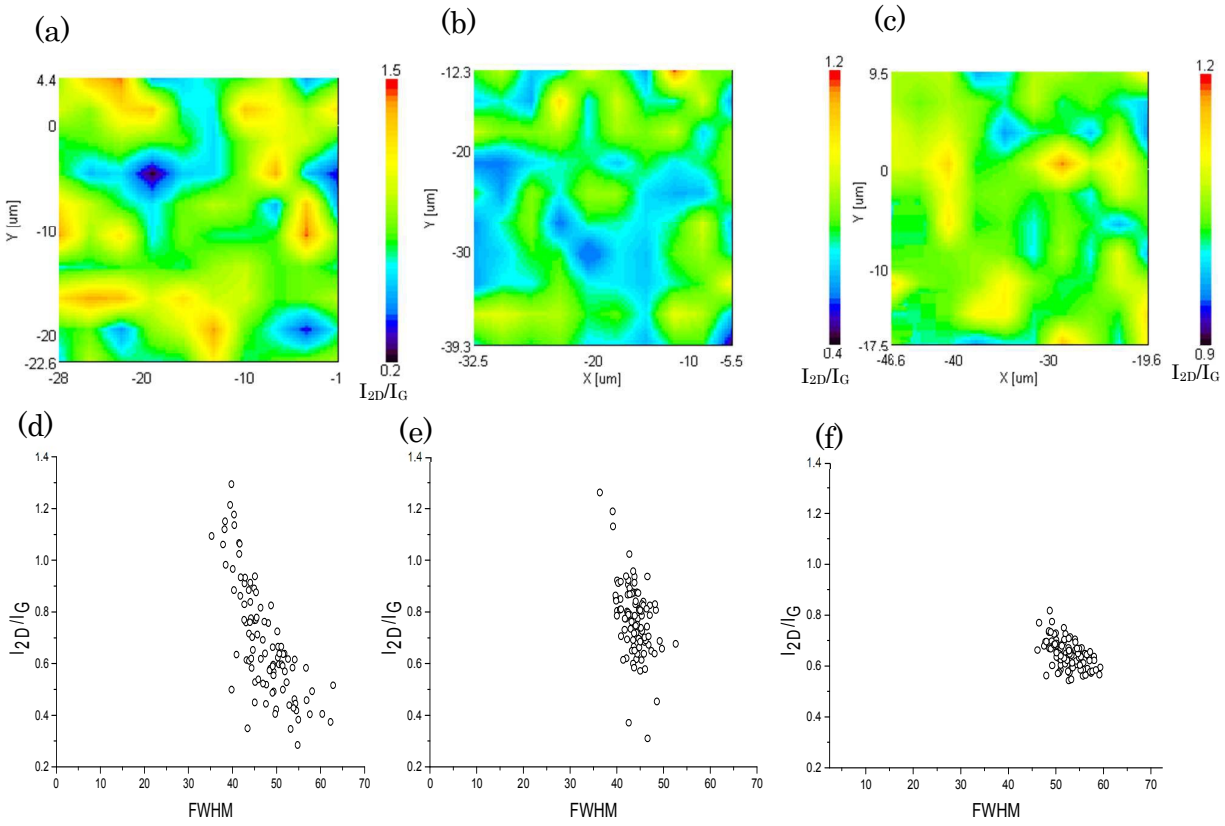

Figure 3, Raman mapping image with variation of deposition time(a-c). Deposition for (a) 5 minutes (b) 15 minutes and (c) 30 minutes.I_{2D}/I_G vs FWHM plot for deposition of (d) 5 minutes, (e) 15 minutes and (f) 30 minutes.

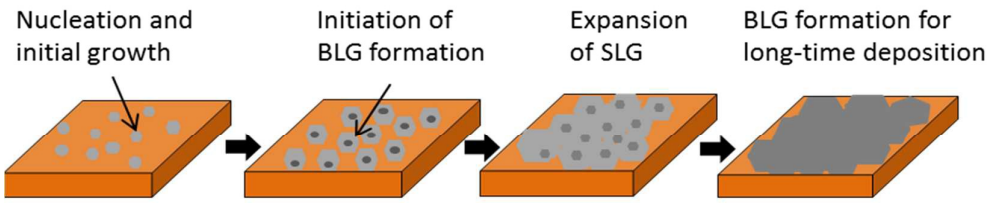

Figure 4,BLG gowth meachnism by suppression of nucleation,(a) Graphene nucleation on Cu,(b)BLG nucleation in the mid of SLG,(c)Extension of coverage of SLG,(d)BLG growth over the Cu substrate and contour plot of BLG and SLG.

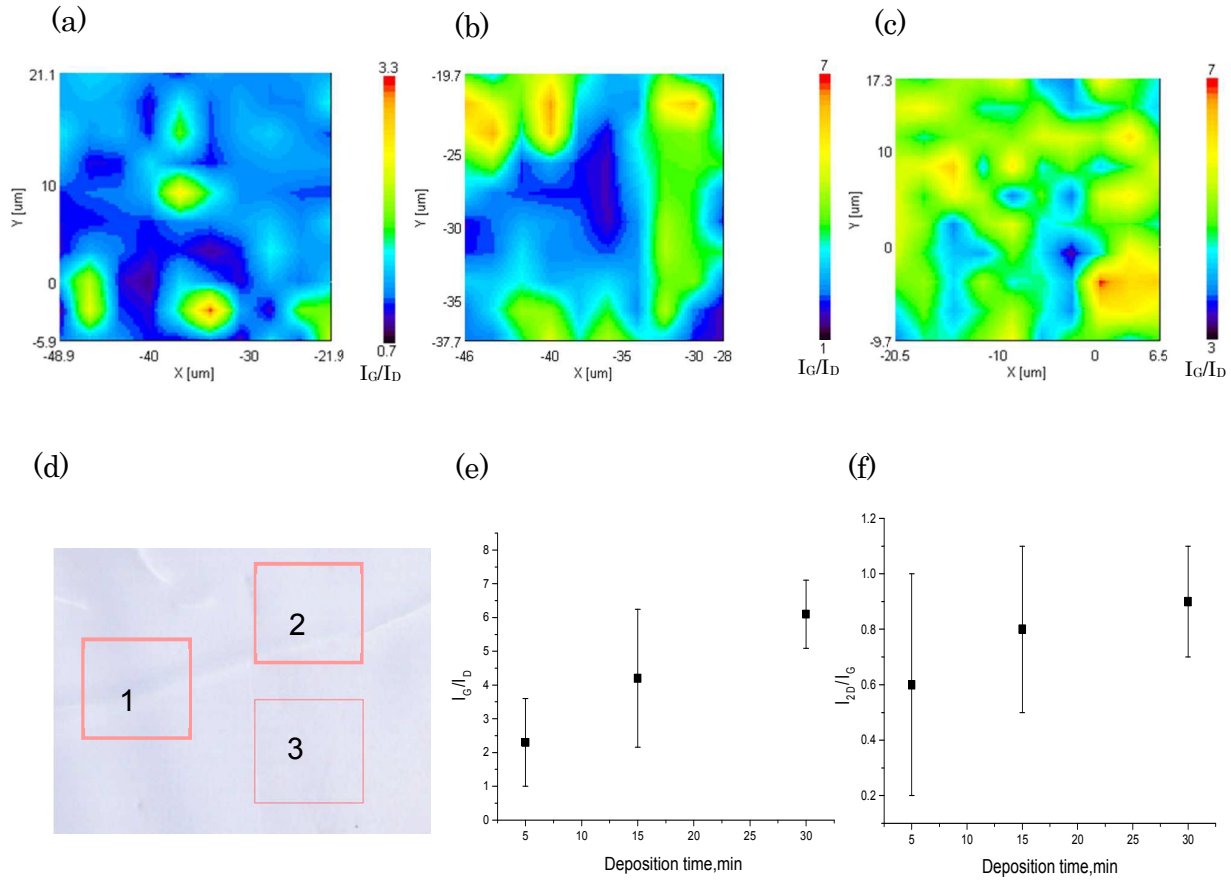

Figure 5, Raman mapping of G/D ratio for different deposition time(a-c); deposition for (a)5 minutes, (b)15 minutes and (c) 30 minutes.(d) Opticalmicroscopic image considering three regions.(e)I_D/I_G vs deposition time,(f)I_{2D}/I_G vs deposition time.

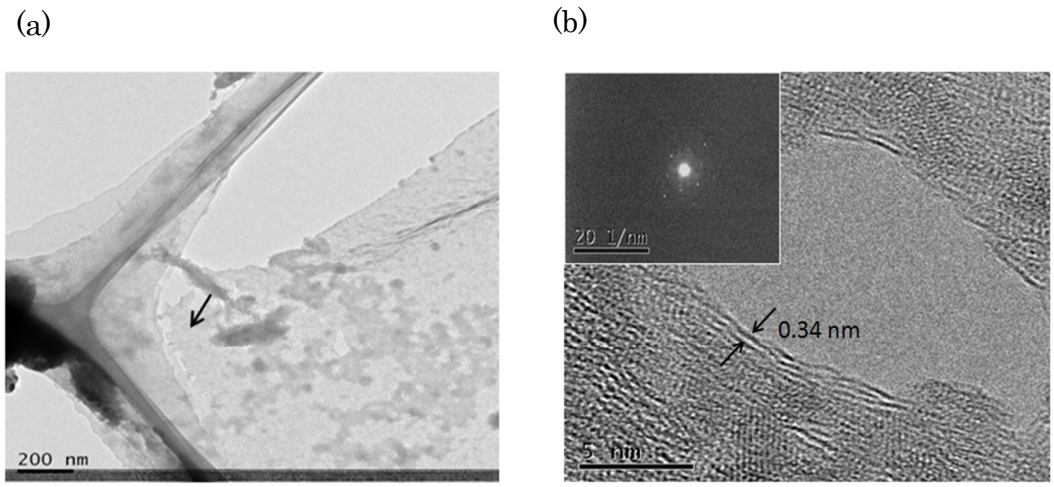

Figure 6,(a) Graphene in TEM grid and (b) As-grown Bi-layer graphene.Inset image shows diffraction pattern of BLG.

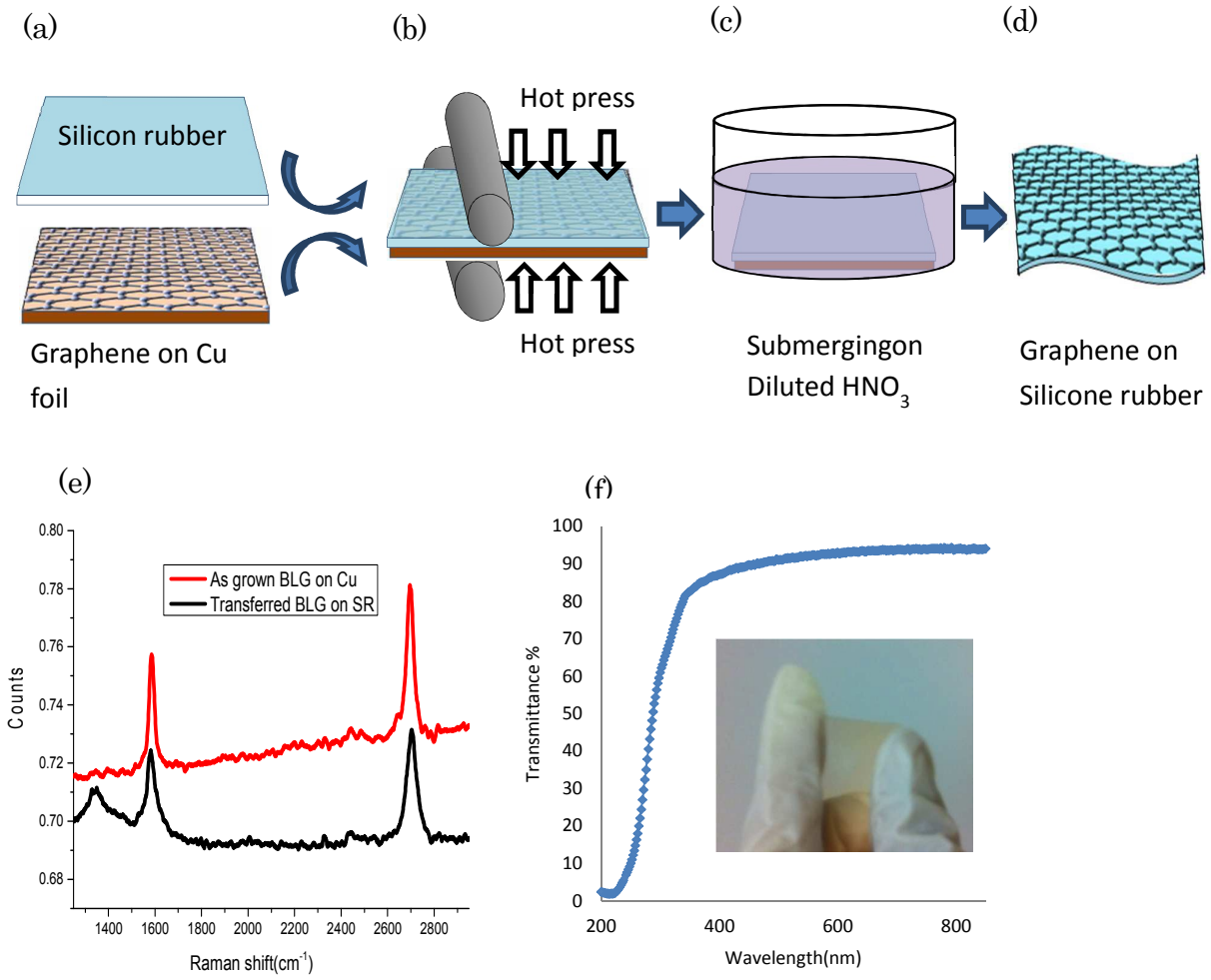

Figure 7, Transfer process of graphene from Cu foil to silicone rubber;(a-b)Graphene on Cu foil and silicone rubber(SR) were hot pressed at moderate temperature and pressure,(c)Cu/BLG/SR was submerged into diluted HNO_3 and (d) final graphene on SR (e)Raman spectroscopy of as-grown graphene on Cu substrate and tranferred BLG on SR and (f) Measured transmittance of bilayer graphene on silicon rubber.Inset image shows tranparent graphene on SR.

Graphical abstract:

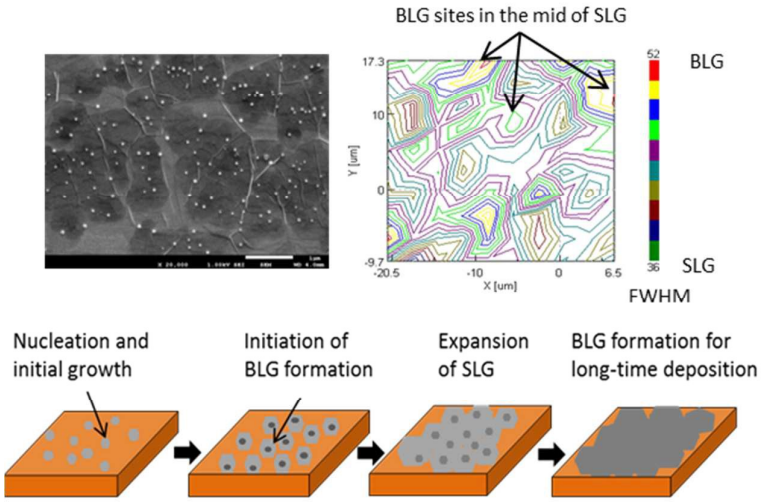

Textual abstract:

Nucleation was controlled and suppressed by two-way carrier gas insertion and continuous bilayer graphene was synthesized from botanical derivative, camphor.